

# Failure time and critical behaviour of fracture precursors in heterogeneous materials

A. Guarino<sup>\*♦</sup>, S. Ciliberto<sup>\*</sup>, A. Garcimartín<sup>‡</sup>,  
M. Zei<sup>★♣</sup> and R. Scorretti<sup>\*♡</sup>

<sup>\*</sup>Ecole Normale Supérieure de Lyon, 46 allée d'Italie, 69364 Lyon, France

<sup>‡</sup>Departamento de Física, Facultad de Ciencias, Universidad de Navarra,  
E-31080 Pamplona, Spain.

<sup>♣</sup>Facoltà di Ingegneria, Università degli Studi di Firenze,  
via S. Marta 4, Firenze, Italia.

## Abstract

The acoustic emission of fracture precursors, and the failure time of samples of heterogeneous materials (wood, fiberglass) are studied as a function of the load features and geometry. It is shown that in these materials the failure time is predicted with a good accuracy by a model of microcrack nucleation proposed by Pomeau. We find that the time interval  $\delta t$  between events (precursors) and the energy  $\varepsilon$  are power law distributed and that the exponents of these power laws depend on the load history and on the material. In contrast, the cumulated acoustic energy  $E$  presents a critical divergency near the breaking time  $\tau$  which is  $E \sim \left(\frac{\tau-t}{\tau}\right)^{-\gamma}$ . The positive exponent  $\gamma$  is independent, within error bars, on all the experimental parameters.

## 1 Introduction

Heterogeneous materials are widely studied not only for their large utility in applications but also because they could give more insight to our understanding of the role of macroscopic disorder on material properties. The statistical analysis of the failure of these materials is an actual and fundamental problem which has received a lot of attention both theoretically [1, 2, 3, 4, 5, 6, 7] and experimentally [8, 9, 10, 11, 12]. When an heterogeneous material is stretched its evolution toward breaking is characterized by the appearance of microcracks before their final break-up. Each microcrack produces an elastic wave which is detectable by a piezoelectric microphone. The microcracks constitute the so called precursors of fracture. It is very well known that these materials subjected to a constant load may break after a certain time, which is a function of the applied load. Many models have been proposed to predict this failure time, but the physical mechanisms remain unclear [3, 4, 13, 14]. Very recently it

has been proposed [15, 16] a model, which explains quite well the failure time of microcrystals [17] and gels [19] submitted to a constant stress load. This model is based on the idea that a nucleation process of a microcrack has to take place inside the materials, in order to form the macroscopic crack. This nucleation process is controlled by an activation law, as the coalescence of a phase into another in a liquid-solid transition. Based on this prediction [16], L. Pauchard et al. [17] found that if a constant load is applied to a bidimensional microcrystal[18], it breaks after a time  $\tau$  given by the equation  $\tau = \tau_o e^{P_o^2/P^2}$ , where  $P$  is the applied pressure, and  $\tau_o$  and  $P_o$  are constants. Bonn et al. [19] found a similar law for gels. Pomeau predicted that for three-dimensional microscopic systems the life-time should be:

$$\tau = \tau_o \exp\left(\frac{P_o}{P}\right)^4 \quad (1)$$

where  $\tau_o$  is a characteristic time and  $P_o$  a characteristic pressure, which mainly depend on the material characteristics, the experimental geometry and temperature. The idea, that the life time of a material might be due to a thermally activated process, has been proposed long time ago by Mogi [20] and Zhurkov [13]. They got a different expression for  $\tau$

$$\tau = \tau_o \exp\left(-\frac{P}{P_o}\right) \quad (2)$$

This equation was accurately checked in many homogeneous materials and it shows a good agreement with experimental data [13]. However it has to be stressed that eq.1 and 2 are certainly first order approximation because they neglect the tensorial nature of crack perturbations and their long range interactions [6]. These ideas are quite interesting and it is important to check experimentally whether they can be applied in heterogeneous materials, such as fiber glass and wood pannels[21]. In two recent papers [9, 10], we have shown that in these materials the microcracks, preceding the main crack form something like a coalescence around the final path of the main crack. The purpose of this paper is to investigate more deeply the behaviour of these materials, and specifically the statistical properties of fracture precursors and their relationships with the failure time. The paper is organized as follows: in section 2 we describe the different experimental settings. In section 3 we study the time failure for the samples submitted to a constant load (3.1) and its statistical properties (3.2). Then we generalize to a time dependent load. In section 4 the statistical behaviour of the fracture precursors is studied as a function of the load features and the geometry. Discussion and conclusions follow in section 5.

## 2 Experimental setups

In order to verify the dependence of the results on the geometry and on the fracture's mode, we used three different experimental setups. We performed

mode-I fracture experiments both with a classical tensile machine (TM) and a high pressure chambers (HPC). In the case of the TM the stress distribution is very simple but, due to moving mechanical parts, we have to deal with a large acoustic noise. In order to avoid noise and to detect reliably microcracks with a weak sound emission, we have designed a set-up in which there are no moving parts except the sample itself, the HPC. Here, the stress distribution is very complicated but numerical calculations[22] show that the experience can be thought of as a Mode-I test with circular symmetry. Finally, we used a flexion-machine to perform mode-I tests.

## 2.1 Samples

Several materials have been used. Most of the runs have been carried out on two fibrous composite materials: chipboard wood panel, which is made of small wood fibers randomly oriented, and different fiberglass panels made of a fiber fabric and an epoxy resin. The Young modulus of the samples is  $1.8 \cdot 10^8 \text{ N/m}^2$  and  $10^{10} \text{ N/m}^2$  for the wood panels and the fiberglass respectively. The Poisson's modulus is  $\nu = 0.35$  for both materials. The longitudinal sound velocity is  $1900 \text{ m/s}$  for wood panels and  $2200 \text{ m/s}$  for fiberglass. The choice of the materials was determined by their features: they consist of small fibers, randomly oriented, and they are elastic and heterogeneous. The geometry of the samples, which depends on the experimental set up used to test it, is described in the following sections.

## 2.2 High pressure chambers (HPC)

A circular wood or fiberglass sample having a diameter of  $22 \text{ cm}$  and a thickness between  $1$  and  $5 \text{ mm}$  is placed between two chambers between which a pressure difference  $P = P_2 - P_1$  is imposed(see fig. 1b). If the deformation of the plate at the center is bigger than its thickness, which is the case here, the load is mainly radial [23, 24]. Therefore, the experience can be thought of as a Mode-I test with circular symmetry. The pressure difference  $P$  supported by the sample is slowly increased and it is monitored by a differential transducer. This measure has a stability of  $0.002 \text{ atm}$ . The fracture pressure for the different tested materials ranges from  $0.7$  to  $2 \text{ atm}$ . We regulate  $P$  by means of a feedback loop and an electronically controlled valve which connects one of the two chambers to a pressurized air reservoir. The time taken to correct pressure variations (about  $0.1$  second) is smaller than the characteristic time of the strain rate. An inductive displacement sensor (Linear Differential Variable Transducer 500HR from PM Instrumentation) gives the deformation at the center of the plate with a precision of about  $10$  microns (the deformation just before fracture is of the order of one centimeter, depending on the material). The apparatus is placed inside a copper box covered with a thick foam layer to avoid both electrical and acoustic noise. Four wide-band piezoelectric microphones (Valpey-Fisher Pinducer VP-1093) are placed on the side of the sample (see fig. 1a,b). The signal is amplified, low-pass filtered at  $70 \text{ kHz}$ , and sent to a digitizing

oscilloscope and to an electronic device which measures the acoustic energy detected by the microphones. The signal captured by the oscilloscope is sent to a computer where a program automatically detects the arrival time of the acoustic emissions (AE) at each microphone. If the signal is detected by more than two microphones, a calculation yields the position of the source inside the sample. A fraction of the detected events are rejected, either as a result of a large uncertainty of the location, or because they are regarded as noise. The mean standard error for the calculated positions is about 6 *mm*, which results mainly from the uncertainty of the arrival time. The electronic device that measures the energy performs the square of the AE amplitude and then integrates it over a time window of 30 *ms*, which is the maximum duration of one acoustic event. The output signal is proportional to the energy of the events, and its value is sent to the computer. The dynamic range for the energy measurement is four decades, and the device is adjusted in such a way that only the strong sound emitted by the final crack saturates it. The global results of the measurements are the following: a list of the positions of microcracks, the strain of the samples and the energy released as a function of the control parameter  $P$ . Further details of the setup are described elsewhere[10, 9, 21, 22].

### 2.3 Tensile Machine (TM)

The experimental apparatus consists of a tensile machine (see fig. 1c) which can apply a maximum force of about 23000 *N*. During the load we measure the applied force  $F$ , the strain, the *AE* produced by microcracks and the time at which the event was detected. The data acquisition set-up is the same used with the HPC. The samples have a rectangular shape of size  $l = 30$  *cm*,  $w = 20$  *cm* and thickness of 2 *mm*. More details of the experimental setup can be found in [25].

### 2.4 Bending-machine (BM)

The apparatus is a three-points flexion machine, fig.2. The rectangular sample lies horizontally with fixed edges and vertical load is imposed in its center. The size of the samples is  $l = 8$  to 22 *cm*,  $w = 1$  to 2 *cm*, and the thickness is 0.2 *cm*. With this setup we only used fiberglass samples. We can load the sample up to 65*Kg* (that is the machine critical load) by minimum steps of 100 *g*. An inductive displacement sensor, similar to the one used in the HPC, has been used to measure the displacement of the center of the sample  $f$ . The sensor is connected to a computer that samples the signal at 1*Hz*. The failure time  $\tau$  is obtained by the analysis of the signal  $f(t)$ ; The uncertainty of  $\tau$  is then 0.5 *s*. No acoustic emissions are measured with this apparatus. More details are described in [26].

### 3 The failure time

The aim of this section is to study the lifetime  $\tau$  of heterogeneous materials and to check whether eq.(1) could be useful in order to predict it. We first investigate  $\tau$  when samples are submitted to a constant load using the *HPC* and the *BM*. Then we consider the case of a time dependent load, and we try to generalize eq.(1).

#### 3.1 Constant load

We first impose a constant strain to our samples (using all the apparatus), as it has been made for crystals[17]. As strain is fixed, every microcrack leads to a pressure decrease: in fact each microcrack weakens the material, so that a lower pressure is needed to keep the strain constant. It follows that if the imposed strain is small enough<sup>1</sup>, the system reaches a stationary state, where the pressure remains constant and no more microcracks are detected[22] (see fig. 3b). One sample was submitted to a large deformation (i.e. close to the critical value) and it did not break after three days. Therefore, at imposed strain, the effect observed in microcrystals is not valid for heterogeneous materials.

On the other hand, if a constant stress is imposed to the system, no matter which apparatus we use, it will break after a certain time which depends on the value of the applied load. This can be done by imposing a constant pressure with the HPC (see fig. 3a) or a constant force with the TM and BM. The reason for this is that after every single microcrack the same load must be endured by the weakened sample, so that it becomes more and more unstable. Using either the TM or HPC, we have submitted several samples to different constant loads  $P$  and we have measured the life-time  $\tau$ . The values obtained are well fitted by eq.(1), that is the exponential function predicted by Pomeau. On the other hand, the life-time expression  $\tau = ae^{-bP}$  proposed by Mogi[20] does not conform to our data[27]. The same law has been found experimentally by Zhurkov[13]. However it's worth noting that his work deals mainly with homogeneous, visco-elastic and plastic materials, whereas the materials we used are heterogeneous and elastic: this could explain why he found a different dependence of  $\tau$  on the imposed load. In fig. 4  $\tau$  is plotted versus  $\frac{1}{P^4}$  in a semilog scale and a straight line is obtained. Fig.4 corresponds to the case of wood samples broken in the HPC, while in fig. 5 we show the points for fiberglass samples broken in the BM. Each point corresponds to the mean value obtained with 20 samples. Even if the load is very small the sample will eventually break, although the life-time can be extremely long. For example, using eq.(1) and the best fit parameters of fig. 4a, one estimates  $\tau \simeq 5000$  s at  $P = 0.43$  atm. Halving the imposed pressure causes  $\tau$  to become extremely large :  $\tau = 4.4 \cdot 10^{37}$  years at  $P = 0.21$  atm).

The value of  $\tau_o$  seems to depend on the geometry and the material but not, within the error bar, on the sample size. In fact, for the circular samples broken

---

<sup>1</sup>it's clear that if the imposed strain has to be smaller than a critical value, at which the sample breaks instantaneously.

with the HPC, we find  $\tau_o = 50.5 \pm 0.2$  s for wood and  $\tau_o = 44.6 \pm 0.2$  s for fiberglass. While in the the BM we find  $\tau_o = 2.5 \pm 0.3$  s and  $\tau_o = 2.7 \pm 0.3$  s for the samples with  $W = 1cm$  and  $W = 2cm$  respectively.

The value of  $P_o$  depends both on the geometry, the size and the material of the sample, and indeed we find  $P_o = 2.91$  atm and  $P_o = 0.63$  atm for fiberglass and wood broken in the HPC. For the fiber glass samples broken with the BM the values of  $P_o$  are  $P_o = 71.1$  kg for  $W = 2$  cm and  $P_o = 35$  kg for  $W = 1$  cm

### 3.2 Statistic of the failure times

It's interesting to study the statistical distribution  $N(\tau)$  of the failure times. This information can give more insight on the physical phenomena.

The main hypothesis of Pomeau is that the failure of a sample is due to the thermal nucleation of one defect. Thus one expects that the failure time  $\tau$  follows a Poisson's distribution. This has been experimentally observed in gels[19]. Conversely, in all the measures made with the HPC and the TM the failure time follows a normal distribution. This is also the case for crystals[17].

This difference can be explained by the fact that in our samples the failure is due to the nucleation and coalescence of a large number of defects, each of one is thermally activated and would eventually follows a Poisson's law, if it were isolated. Numerical simulations and analytical calculations seem to confirm this idea[28, 29, 30].

In the case of the experiments performed with the BM, the failure time distribution  $N(\tau)$  seems not to follow a Poisson's law nor a normal distribution, fig. 6a. In this case we observed that the cumulative distribution

$$Q(\tau) = \frac{\int_0^\tau N(t)dt}{\int_0^\infty N(t)dt}$$

is best fitted by the sum of two exponentials, fig.6b. We believe that this is due to the fact that the two components of these samples (the resine and the texture of glass fibers) give rise to different characteristic times. We think that this "separation effect" is observed only with the BM because of the small size of the samples.

### 3.3 Time dependent load

In order to find a law that holds for a time dependent imposed stress, we intend to generalize the eq.(1). If the pressure  $P$  changes with time, it is reasonable to consider the entire history of the load. Therefore we consider that

$$\frac{1}{\tau_o} \exp \left[ - \left( \frac{P_o}{P} \right)^4 \right]$$

is the density of damage per unit time, where  $\tau_o$  and  $P_o$  are fitting parameters obtained in the constant load case. The certitude of breaking is obtained after

a time  $\tau$  such that:

$$\int_0^\tau \frac{1}{\tau_o} \exp \left[ - \left( \frac{P_o}{P} \right)^4 \right] dt = 1 \quad (3)$$

where  $\tau_o$  and  $P_o$  have the previously determined value. Notice that this equation is equivalent to eq.(1) when a constant pressure is applied.

To check this idea, we have applied the load to the sample (using the HPC) following different schemes. We have first applied successive pressure plateaux in order to check whether memory effects exist. In fig. 7a the pressure applied to the sample is shown as a function of time. A constant load has been applied during a certain time  $\tau_1$ , then the load is suppressed and the same constant load is applied again for a time interval  $\tau_2$ . The sample breaks after a loading a time  $\tau_1 + \tau_2$  which is equal to the time needed if the same load had been applied continuously without the absence of load during a certain interval. Therefore a memory of the load history exists. The life-time formula (eq. 3) is also valid if different constant loads are applied successively (fig. 7b). This concept can explain the violation of the Kaiser effect in these materials[10].

If the load is not constant, the life-times resulting from the proposed integral equation are still in good agreement with experimental data. A load linearly increasing at different rates  $A_p$  has been applied to different samples. The measured breaking times are plotted in fig. 8 along with a curve showing the values computed from eq.3. Even if a quasi-static load is applied erratically (fig. 7c), the calculated life-time agrees with the measured one. These experiments show that eq. 3 describes well the life-time of the samples submitted to a time dependent pressure.

### 3.4 The dependence of $\tau$ on the temperature

The question is to understand why eq.(1) and (3) works so well for a three dimensional heterogeneous material. Indeed, in the Pomeau formulation [16]

$$P_o = G \left( \frac{\eta^3 Y^2}{KT} \right)^{1/4} \quad (4)$$

where  $Y$  is the Young modulus,  $T$  the temperature,  $K$  the Boltzmann constant and  $\eta$  the surface energy of the material under study.  $G$  is a geometrical factor which may depend on the experimental geometry, on defect shape and density.

In our experiment with HPC, we found  $P_o = 0.62 \text{ atm}$  for wood, which has  $Y=1.8 \cdot 10^8 \text{ N/m}^2$ , and  $P_o = 2.91 \text{ atm}$  for fiberglass, which has  $Y = 10^{10} \text{ N/m}^2$ . Thus the ratio between the values of  $P_o$  found for the two materials is closed to the ratio of the square root of their Young modula.

In contrast temperature does not seem to have a strong influence on  $\tau$ . In fact we changed temperature, from  $300K$  to  $380K$  which is a temperature range where the other parameters,  $Y$  and  $\eta$ , do not change too much. For this temperature jump one would expect a change in  $\tau$  of of about 50% for the

smallest pressure and of about 100% for the largest pressure. Looking at fig. 8 we do not notice any change of  $\tau$  within experimental errors which are about 10%. In order to maintain the change of  $\tau$  within 10% for a temperature jump of  $80K$  one has to assume that the effective temperature of the system is about  $3000K$ . Notice that this claim is independent on the exact value of the other parameters and  $G$ .

These observations seem to indicate that the nucleation process of microcracks is activated by a noise much larger than the thermal one. Such a large noise can be probably produced by the internal random distribution of the defects in the heterogeneous materials that we used in our experiments. This internal random distribution of material defects evolves in time because of the appearance of new microcracks and the deformation of the sample. Therefore this internal and time dependent disorder of the material could actually be the mechanism that activates the microcrack coalescence and play the role of a very high temperature. Numerical simulations and analytical calculations, which we performed in fuse networks, confirm this hypothesis[28, 29, 30]. Similar conclusions on the role of disorder in the crack activation processes have been reached by other authors[31, 6]. The experimental test of these models is a very important point which merits to be deeply explored in the future.

## 4 Statistical behavior of fracture precursors

When a constant pressure is applied to the sample using the HPC, the acoustic emissions of the material are measured as a function of time. We find that the cumulative acoustic energy  $E$  diverges as a function of the reduced time  $\frac{\tau-t}{\tau}$ , specifically  $E \propto (\frac{\tau-t}{\tau})^\gamma$  with  $\gamma = 0.27$  (see Fig. 10). Notably, the exponent  $\gamma$ , found in this experiment with a constant applied pressure, is the same of the one corresponding to the case of constant stress rate [9]. Indeed it has been shown [9, 10] that if a quasi-static constant pressure rate is imposed, that is  $P = A_p t$ , the sample breaks at a critical pressure  $P_c$  and  $E$  released by the final crack precursors (microcracks) scales with the reduced pressure or time (time and pressure are proportional) in the following way:

$$E \propto \left( \frac{P_c - P}{P_c} \right)^\gamma = \left( \frac{\tau - t}{\tau} \right)^\gamma \quad (5)$$

where  $\tau = P_c/A_p$  in this case. Thus it seems that the real control parameter of the failure process is time, regardless of the fact that either a constant pressure rate or a constant pressure is applied. In the case of constant load rate ( $P = A_p t$  or  $u = Bt$ ) the system has not a characteristic scale of energy or time: the histogram  $N(\varepsilon)$  of the released energy and the histogram  $N(\delta t)$  of the elapsed time  $\delta t$  between two consecutive events reveal power laws, i.e.  $N(\varepsilon) \sim \varepsilon^{-\alpha}$  and  $N(\delta t) \sim \delta t^{-\beta}$ . The exponents  $\alpha$ ,  $\beta$  and  $\gamma$  do not depend on the load rate  $A_p$  or  $B$ [9, 10]. Power laws for similar magnitudes are found experimentally on cellular glass[12], and numerically in a related process, the dielectric breakdown[32]. The value of the exponents are not too different. We are interested in studying the



exponents in different geometries and when a constant (creep test), cyclic or erratic load are imposed. To check the dependence of  $\alpha$ ,  $\beta$  and  $\gamma$  on the geometry we used the TM. The force applied to the sample is slowly and constantly increased till the sample fails. During the loading we measure the applied force  $F$ , the strain, the AE produced by microcracks and the time at which the event was detected.

#### 4.1 The dependence of $\alpha$ and $\beta$ on the load features

In the experiments performed with the HPC, power laws are obtained for the distributions of  $\epsilon$  and of  $\delta t$ . As an example of two typical distributions obtained at constant imposed pressure, we plot in fig 9a) and 9b)  $N(\delta t)$  and  $N(\delta \epsilon)$  respectively. The exponents of these power laws ( $\alpha_c$  for energies and  $\beta_c$  for times) depend on  $P$ . In fig. 9c,  $\alpha_c$  and  $\beta_c$  are plotted versus  $P$ . Note that both exponents grow with pressure. We observe that the rate of emissions increases with pressure, so that the weight of big values of  $\delta t$  decreases. This explains the fact that  $\beta_c$  grows with pressure. We have compared the histograms of energy  $\epsilon$  for several pressures, and we noticed that the number of high-energy emissions is almost the same, while the number of low-energy emissions increase with pressure, so that the exponent  $\alpha_c$  increases as well. Moreover, as the pressure increases, the exponents  $\alpha_c$  and  $\beta_c$  attain the values  $\alpha = 1.9 \pm 0.1$  and  $\beta = 1.51 \pm 0.05$  obtained in the case of a constant loading rate[10]. We imposed to the sample a erratic and an cyclic load, which are plotted as a function of time in figure 11a and 11b respectively. Power laws are obtained for the distributions of  $\epsilon$  and for  $\delta t$ . The exponents of these power laws do not depend on the load behavior; their value is the same of that at constant loading rate. These and previous results [9, 10], allows us to state that if  $\frac{dP}{dt} \neq 0$ , the histograms of the released energy  $\epsilon$  and of the time intervals  $\delta t$  do not depend on the load history. The fact that  $\alpha$  and  $\beta$  do not depend on  $\frac{dP}{dt}$  seems to be in contrast with the fact that  $\alpha_c$  and  $\beta_c$  depend on  $P$ . This result can be interpreted by considering that the microcracks formation process is not the same when  $\frac{dP}{dt} = 0$  and  $\frac{dP}{dt} \neq 0$ . In the former case, imposed constant  $P$ , the mechanism of microcrack nucleation is the dominant one and the nucleation time depends on pressure. In the other case,  $\frac{dP}{dt} \neq 0$ , the dominant mechanism is not the nucleation but the fact that, when pressure increases as a function of time, several parts of the sample may have to support a pressure larger than the local critical stress to break bonds. The fact that at high constant pressure  $\alpha_c$  and  $\beta_c$  recover the value  $\alpha_c$  and  $\beta_c$  has a simple explanation. Indeed, in order to reach a very high pressure  $P_h$ ,  $\frac{dP}{dt}$  is different from zero for a time interval which is comparable or even larger than the time interval spent at constant pressure  $P_h$ . Thus at high constant pressure the system is close to the case  $\frac{dP}{dt} \neq 0$ .

#### 4.2 The dependence of $\gamma$ on the load features

The measures performed with the HPC imposing an erratic and a cyclic pressure, plotted respectively in fig. 11a and 11b, allow us to check the dependence

of  $\gamma$  on the history of the sample, i.e. on the behavior of the imposed pressure. The cumulated energy  $E$  for the erratic and the cyclic pressure, shown in fig 11a and 11b as a function of  $t$ , is plotted in log-log scale as a function of the reduced parameter  $\frac{\tau-t}{\tau}$  in fig 12a and 12b respectively. We observe that, in spite of the fluctuations due to the strong oscillations of the applied pressure, near the failure the energy  $E$ , as a function of  $\frac{\tau-t}{\tau}$ , is fitted by a power law with  $\gamma \simeq 0.27 \pm 0.02$ . In fig.12c (reproduced in fig.10 for the sake of clearness),  $E$  measured when a constant pressure is applied to the sample is plotted as a function of  $\frac{\tau-t}{\tau}$ . A power law is found in this case too [21]. The exponent  $\gamma$  is, within error bars, the same in the three cases. Hence it seems not to depend neither on the applied pressure history nor on the material[9, 10, 21].

Further, experiments made with the TM show that  $\gamma$  is independent on the geometry. In fact we observe that the behavior of the energy near the fracture as a function of  $(\frac{\tau-t}{\tau})$  is still a power law of exponent  $\gamma \simeq 0.27$ , as shown in figure 12d.

## 5 Discussion and conclusions

We presented the results of experiments regarding fracture of heterogeneous materials (chipboard and fiberglass). When these materials are submitted to a strain, one observes acoustic emissions (precursors) before the samples fails. We have measured the acoustic emissions and the lifetime  $\tau$  of the samples.

We have shown that eq.(1) proposed by Pomeau predicts well the functional dependence of  $\tau$  on the applied load. However the original Pomeau's theory is unable to explain some features that are observed in our experiments, in microcrystals[17] and gels[19]. In fact eq.(1) is based on the idea that the fracture is due to the nucleation of *one* preexisting defect, which is thermally activated. We have shown that in our experiments the fracture is due to the nucleation and coalescence of a large number of defects, as confirmed by the presence of acoustic emissions and the shape of the statistical distribution of lifetimes. Moreover, we found that the lifetimes are not affected, within the experimental errors (20 %), by the temperature. We have calculated that in order to estimate the measured lifetimes, the temperature  $T$  to insert in eq.1 and in eq.4 should be about 3000 K. Similar results have been found in 2D crystals[18] and gels, where the temperature  $T$  to insert in eq.(3) should be about  $1000K < T < 2500K$  and  $T_{eff} > 10^{10}K$  respectively. As for wood and fiberglass, also in gels the lifetime  $\tau$  of the sample is not influenced, in the limit of experimental errors, by a variation of the temperature  $T$  from 20 to 90 °C. In contrast, experiments on 2D-crystals [17] show that  $\tau$  depends on  $T$ .

To explain these points we propose to modify in a statistical model the one of Pomeau. In this revised model the failure of the sample is due to the nucleation and coalescence of a certain number of defects, each of which is thermally activated. The parameters  $Y$ ,  $\eta$  and  $T$  of eq.(3), become average parameters, which keep into account that the interaction between defects have

a tensor nature and are long range [6]. To explain the fact that the thermal temperature has a minor influence on the lifetime, we suppose that the strong time-dependent fluctuations of the internal forces induced by the heterogeneity (defects, microcracks ...) can be considered as a sort of noise. Thus  $T$  depends on the thermal temperature but mainly on the disorder in the medium. In this way the heterogeneity of the material enhances thermal fluctuations so that the nucleation time of defects becomes of the order of the measured ones. Recently Arndt *et al.* reached a similar conclusion[31] using a different approach, which is coherent with the generation of a time dependent distribution of the microcrack ensemble [6]. Numerical simulation that we have performed on a very simple model[29, 30] are in agreement with these results. This model allows us to generalize eq.(1) to the case of a time dependent load, and to explain the violation of the Kaiser effect in these materials.

We also studied the statistical properties of the fracture precursors. We have found that the histograms of the energy and of time between two consecutive AE follow power laws of exponents  $\beta$  and  $\alpha$  respectively. In proximity of the fracture the cumulated energy follows a power law, typical of phase transitions. Notably, the critical exponent  $\gamma$  seems to be independent on the geometry and the applied load. Indeed if AE is considered as a susceptibility it is not easy to put together the observed critical divergency with a nucleation process. Probably the standard phase transition description can be only partially applied to failure because of the intrinsic irreversibility of the crack formation.

## 6 Acknowledgements

We thank P. Metz, M. Moulin and F. Vittoz for very useful technical assistance.

## References

- [1] H. J. Hermann, S. Roux, *Statistical Models of Disordered Media*, (North Holland, Amsterdam), 1990.
- [2] D. Sornette and K. Vanneste, Phys. Rev. Lett., **68**, (1992) 5.
- [3] Shah S. P. *Toughening Mechanisms in Quasi Brittle Materials*, Kluwer Academic Publisher (1991).
- [4] Dieter G., *Mechanical Metallurgic*, Mc Graw Hill, (1988).
- [5] Atkinson B. K., *Introduction to fracture mechanics*, Academic Press (1989).
- [6] O. Naimark, M. Davydova, O.A. Plekhov, S.V. Uvarov, *Computers and Structures*, **76** (2000) 67-75.
- [7] A. Politi, M. Zei, Phys. Rev. E 63,056107 (2001).

- [8] J.C. Anifrani, C. Le Flo'h, D. Sornette, B. Souillard, *J. Phys. I France* **5**, 631 (1995).
- [9] Garcimartín A., Guarino A., Bellon L. and Ciliberto S., *Phys. Rev. Lett.* **79**, 3202-3205 (1997).
- [10] Guarino A., Garcimartín A. and Ciliberto S., *European Physical Journal B*, **6**, 13-24 (1998).
- [11] Stead D. and Szczepanik Z., Acoustic emission during uniaxial creep in potash. *Fifth conference on acoustic emission/ microseismic activity in geologic structures and materials*, Pennsylvania State Univ., 97-111 (1991).
- [12] Maes C. Van Moffaert A., Frederix H. and Strauven H., *Phys. Rev. B* **57** 9, 4987-4990 (1998).
- [13] S. N. Zhurkov, *Int. J. Fracture*, v. 1, p. 311 (1965)
- [14] Lawn B., *Fracture of brittle Solids*, Cambridge University Press (1993).
- [15] Gobulović L. and Feng S., *Pys. Rev. A*, **40**, 5223-5227, 10 (1991).
- [16] Pomeau Y., *C. R. Acad. Sci. Paris*, vol. **314** II, 553-556 (1992), (in French).
- [17] Pauchard L. and Meunier J., *Phys. Rev. Lett.* **70** 23, 3565-3568 (1993).
- [18] The thickness of the crystal is just a few molecular layers.
- [19] Bonn D., Kellay H., Prochnow M., Ben-Djemaa K. and Meunier J., *Sciences*, vol. **280**, pp 265-267 (1998).
- [20] Mogi K., *Bull. Earth Res. Inst. Tokyo* **40**, 125- (1962).
- [21] Guarino A., Garcimartín A. and Ciliberto S., *Europhysic Lett.*, vol **47**(4), 456-461 (AUG 1999).
- [22] A. Guarino, *Propriété statistiques des précurseurs de la fracture*, Thèse de doctorat Ecole Normale Supérieure de Lyon (1998).
- [23] L.D. Landau, E.M. Lifshitz, *Theory of elasticity*, Course of Theoretical Physics vol. 7, Pergamon, London (1959).
- [24] S.P Timoshenko, S. Woinowsky-Krieger, *Theory of plates and shells*, McGraw-Hill, Engineering Mechanics Series, New York (1959).
- [25] J.F. Boudet, S. Ciliberto, V. Steinberg, *J. Phys. II*(1996), 1493. J.F. Boudet, S. Ciliberto, *Physica D*, 142 (2000), 317
- [26] M. Zei, *Fractures en matériaux hétérogènes*, Thèse de doctorat Ecole Normale Supérieure de Lyon (2000).

- [27] Several functions with many free parameters have been proposed in order to fit the dependence of the sample life time on the applied stress. Among the fitting functions, which are supported by a microscopic physical mechanism we show in fig. 4a the two functions which give the best fit of our data.
- [28] S. Roux, *Phys. Rev. E* **62**, 6164 (2000)
- [29] S. Ciliberto, A. Guarino and R. Scorretti, *Physica D*, **158** (2001) 83-104.
- [30] R. Scorretti, S. Ciliberto and A. Guarino, *Europhysics letters*, **55**(5), pp. 626-632 (2001).
- [31] P. Arndt and T. Nattermann, *Phys. Rev. B*, vol **73**, 134204 (2001)
- [32] O. Pla and F. Guinea, *Phys. Rev. A*, vol. **42**(10), 6270-6273 (NOV 1990).

Correspondence should be addressed to S. Ciliberto (e-mail: sergio.ciliberto@ens-lyon.fr)

Actual address:

♥ Ecole Centrale de Lyon, 36 avenue Guy de Collongue, 69131 Ecully, France

★ SPCSI, CEA-Saclay, 91191 Gif-sur-Yvette Cedex, France

♦ Université de la Polynésie Française, Jeune Equipe Terre Ocean, BP 6570, FAA'A-Tahiti, French Polynesia

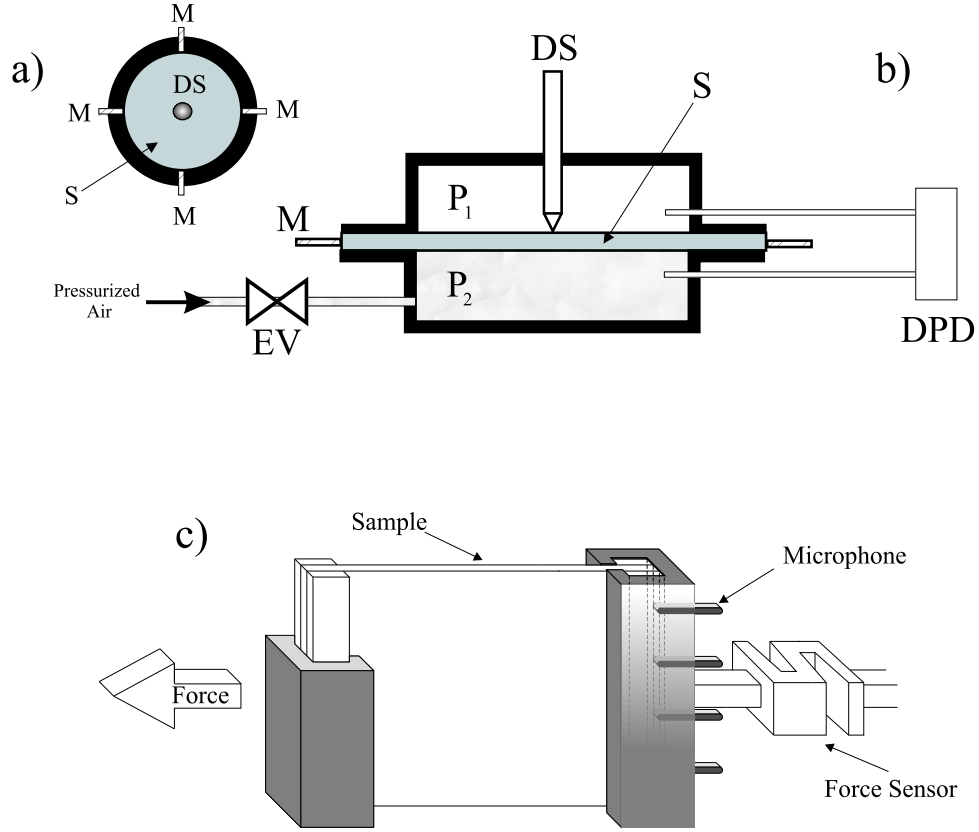


Figure 1: **a, b)** Sketch of the high pressure chamber (HPC) apparatus. S is the sample, DS is the inductive displacement sensor (which has a sensitivity of the order of  $1\ \mu\text{m}$ ). M are the four wide-band piezoelectric microphones.  $P=P_1-P_2$  is the pressure supported by the sample. P is measured by a differential pressure sensor DPD( sensitivity 0.002 atm). EV is the electronic valve which controls P via the feedback control system Ctrl . **c)** Sketch of the tensile machine. An uniaxial force, which is measured by a piezoresistive sensor, is applied to the sample by a stepping motor. Four wide-band piezoelectric microphones measure the acoustic emissions emitted by the sample. Experiments have been done using rectangular (20 x 29 cm) wood samples of 4 mm thickness. The whole apparatus is surrounded by a Faraday screen.

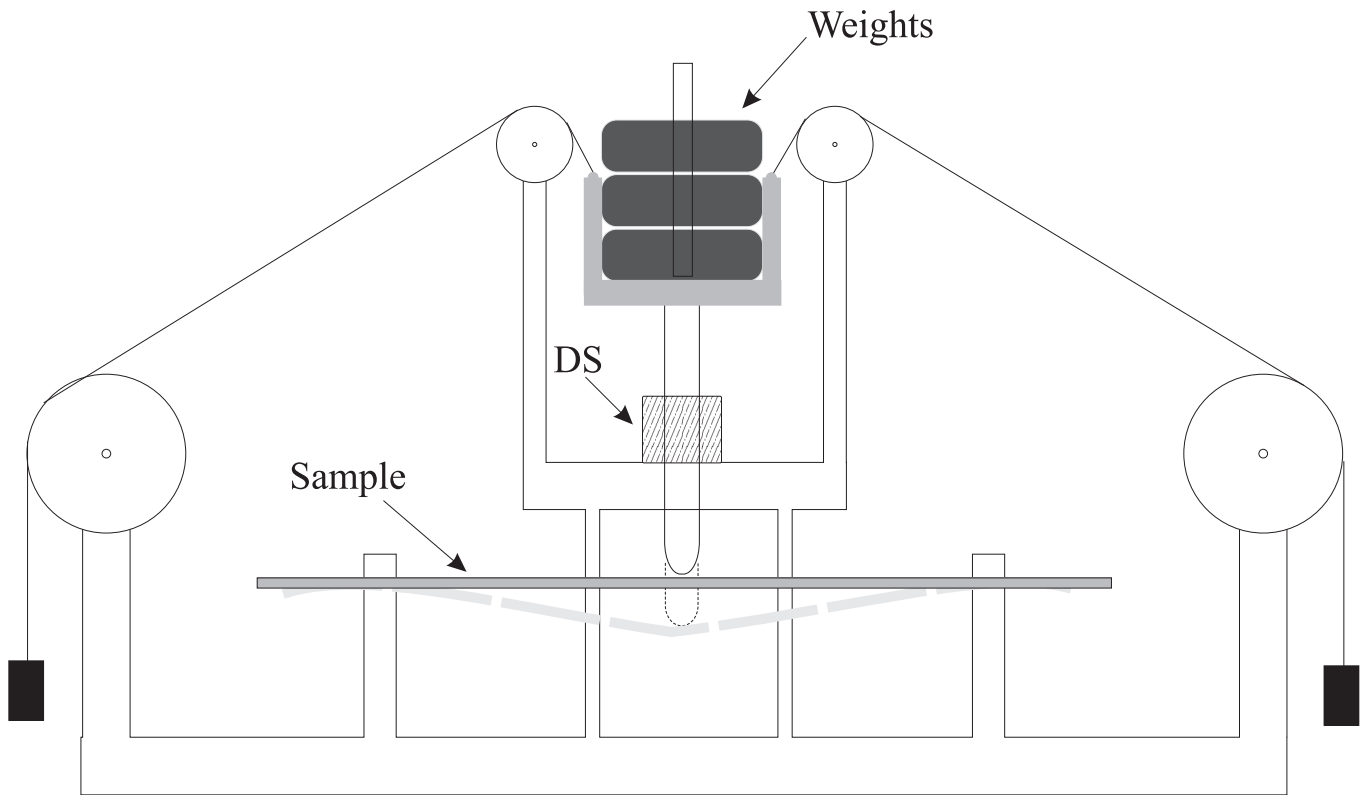


Figure 2: The bending machine (BM). A vertical force is imposed in the center of the sample by using weights (up to  $65\text{ Kg}$ ), so that the sample is broken by bending. The edges of the sample can be clamped or free. The displacement is measured by the sensor DS.

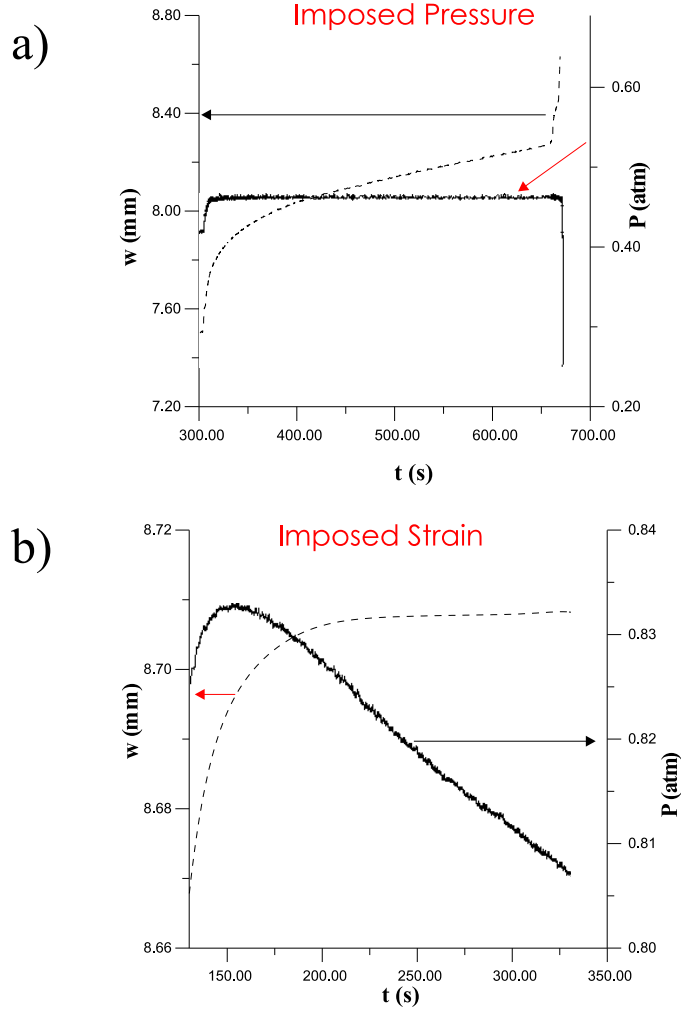


Figure 3: A sample is submitted to a constant load with the HPC. During the load we measure the pressure (continuous line) and the deformation of the sample in its center (dashed line). (a) A constant pressure is imposed to the sample. The deformation increases continuously - even after that the pressure has reached a constant value - till the sample fails. (b) A constant deformation is imposed to the sample. In this case, after a transient period, the pressure decreases till the system reaches a stationary state (not shown in this picture).



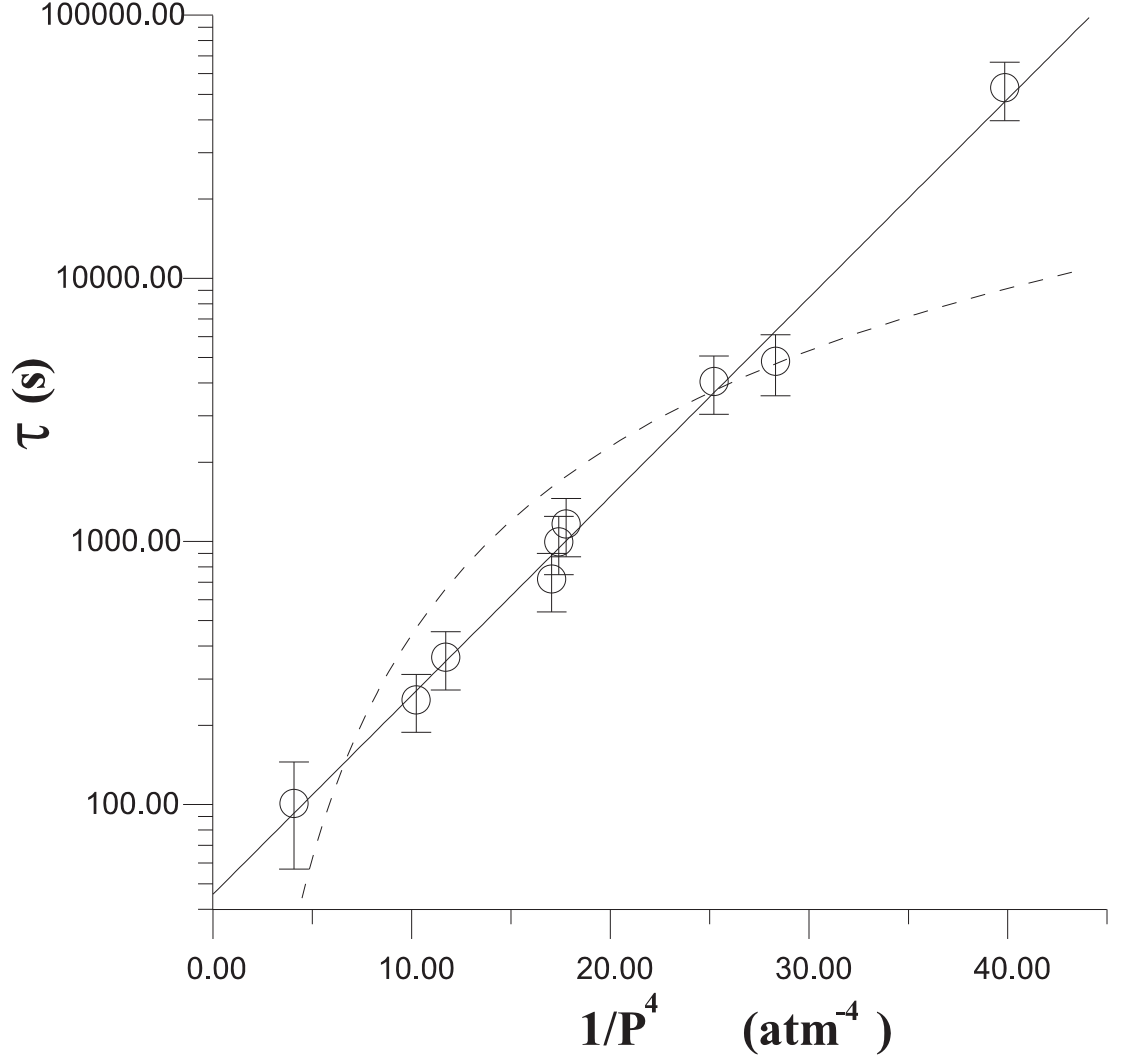


Figure 4: Measurements on wood samples. The time  $\tau$  needed to break the wood samples under an imposed constant pressure  $P$  is here plotted as a function of  $1/P^4$  in a semilog scale. The dashed line represents the solution proposed by Mogi [20] ( $\tau = ae^{-bP}$ ). The continuous line is the solution proposed by Pomeau for microcrystals ( $\tau = \tau_o e^{(P_o/P)^4}$ ). In the plot  $\tau_o = 50.5$  s and  $P_o = 0.63$  atm. Every point is the average of 10 samples. The error bar is the statistical uncertainty. For the fiberglass samples, we find  $\tau_o = 44.6$  s and  $P_o = 2.91$  atm.

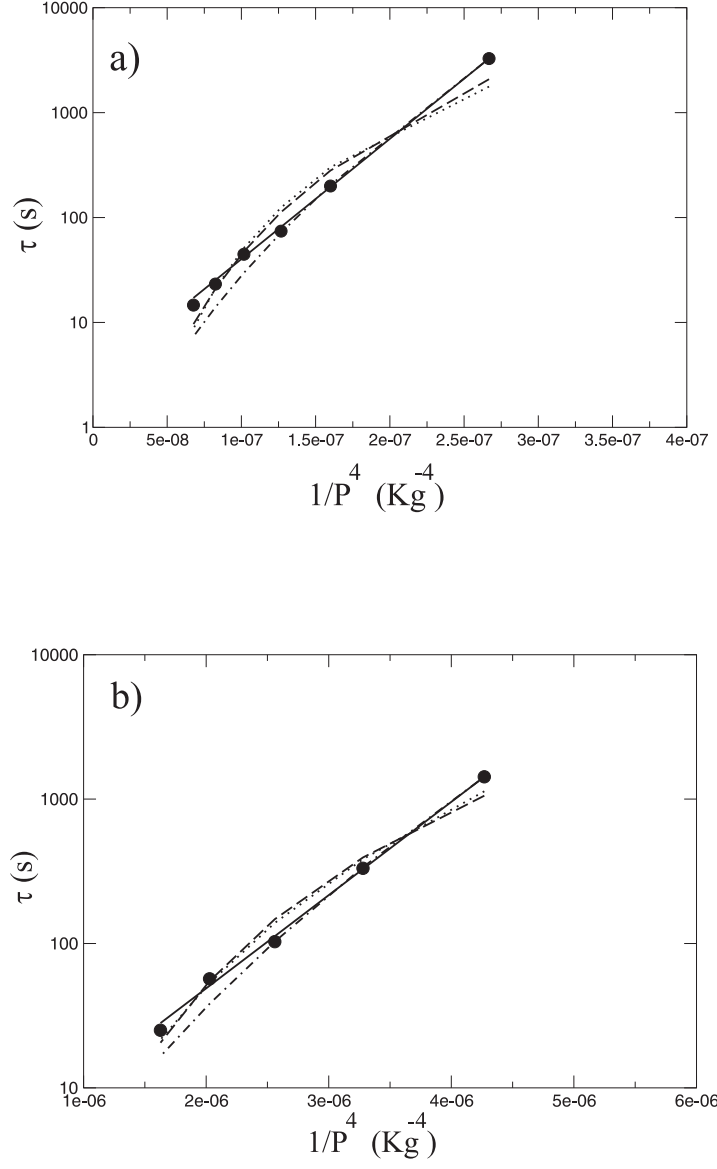


Figure 5: Failure time  $\tau$  of the samples in fiberglass broken with the FM (clamped edges). The sample's size are  $22 \times 2 \times 0.2 \text{ cm}$  (a) and  $22 \times 1 \times 0.2 \text{ cm}$  (b). Each point represents the mean value of 20 measures. Lines represent the best fit with  $\tau = \tau_o \exp\left(\frac{P}{P_c}\right)^4$  (solid line),  $\tau = \tau_o \exp\left(\frac{P}{P_c}\right)^2$  (dashed-dotted line),  $\tau = A \exp(-bP)$  (dotted line), and  $\tau = A P^{-b}$  (dashed line).

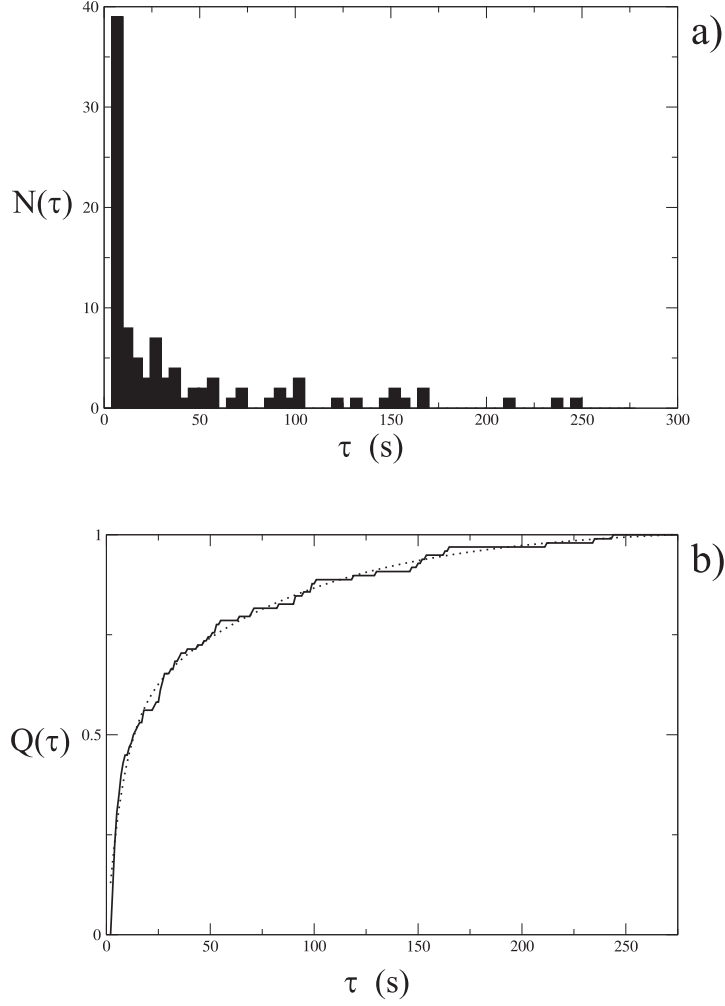


Figure 6: Distribution of the lifetimes  $\tau$  of 100 samples in fiberglass broken with the BM (clamped edges) with a load  $P = 54 \text{ Kg}$ . The sample's size are  $22 \times 2 \times 0.2 \text{ cm}$ . a) The histogram of  $\tau$  shows that the distribution of lifetimes is not gaussian. b) The cumulative distribution  $Q(\tau) = \frac{\int_0^\tau N(t)dt}{\int_0^\infty N(t)dt}$  (solid line) is best fitted by the sum of two exponential terms (dotted line).

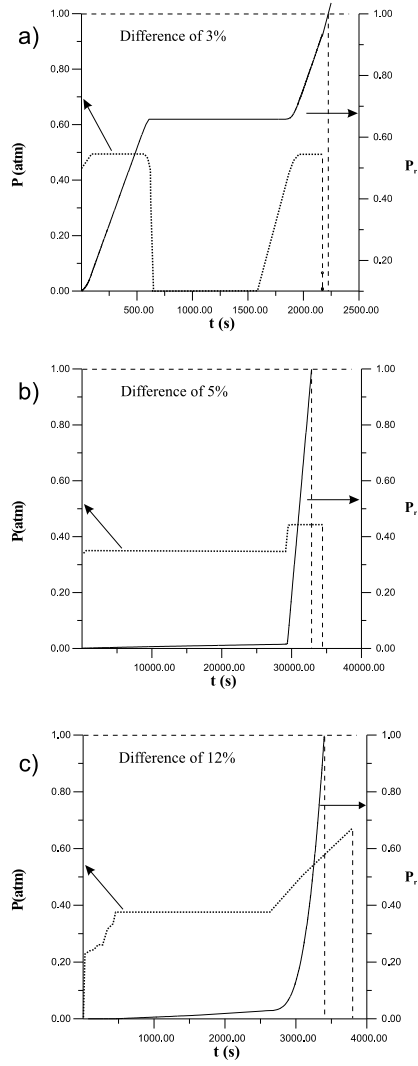


Figure 7: The imposed time dependent pressure (bold dotted line) is plotted as a function of time in the case of wood samples. The continuous line is the integral in time of the function  $f(P) = \frac{1}{\tau_0} e^{-P^4/P^4}$ . On the basis of eq. 3 the predicted breaking time  $\tau$  is obtained when the integral of  $f(P)$  is equal to 1. The horizontal distance between the two vertical dashed lines in each plot represent the difference between the predicted and the measured breaking time. In **a)** a constant pressure has been applied during about 700 s, then the load is suppressed and then the same constant load is applied again. The difference between the life-time predicted by (eq. 3) and the experimental result is of 3%. **b)** Here two pressure plateaux of different value are successively applied to the sample. The difference between the measured and the predicted life-time is of 5%. In **c)** an erratic pressure is applied to the sample. Here the error is of 10%.

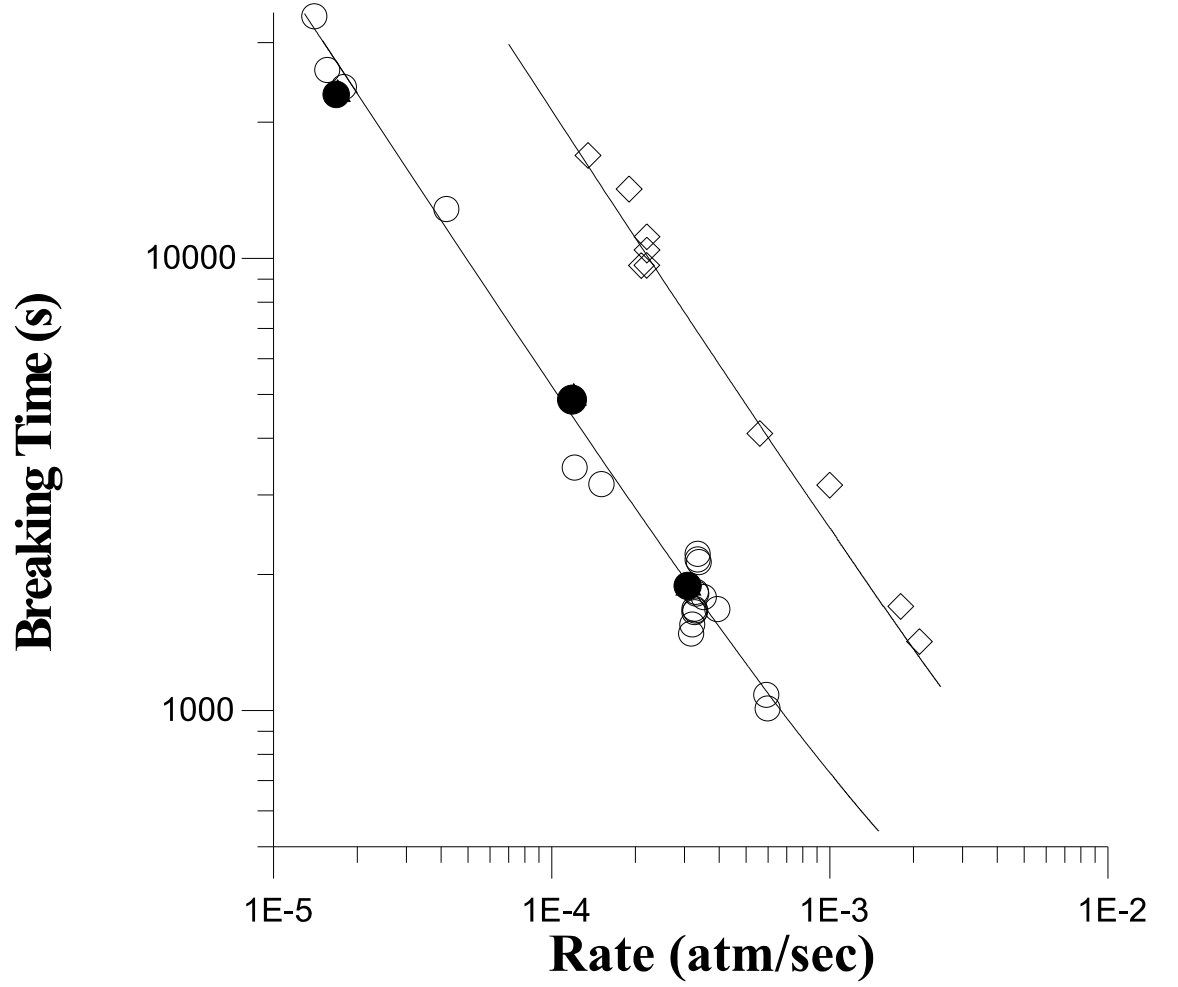


Figure 8: A load linearly increasing at different rates  $A_p$  has been applied to different samples. The measured breaking times are plotted as a function of  $A_p$  in a loglog scale; circles and squares represent the measures on wood and fiberglass samples respectively at  $T=300\text{ K}$ . Bold circles represent measures on wood samples at  $T=380\text{ K}$ . The lines are the life time calculated from eq.3 using the best fit values for  $P_o$  and  $\tau_o$ . These experiments show that eq. 3 describes well the life-time of the samples submitted to a time dependent pressure.

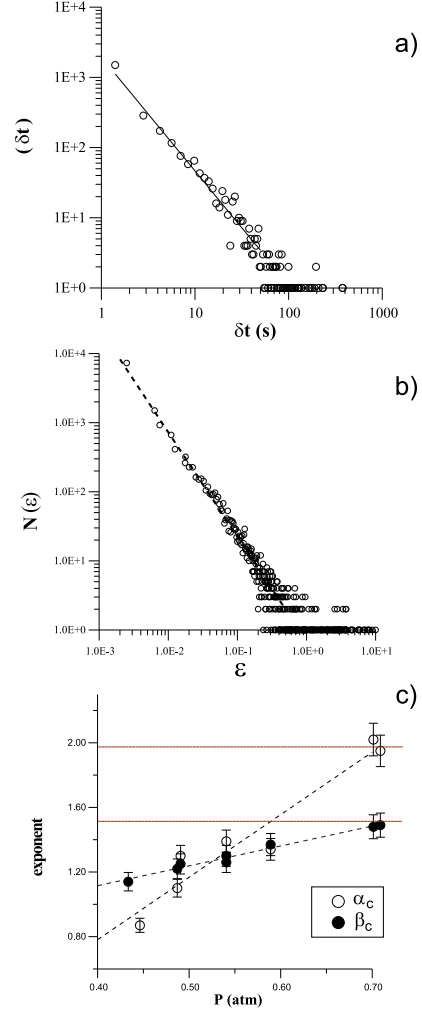


Figure 9: **a,b)** Two typical time  $\delta t$  and energy  $\varepsilon$  distributions obtained at imposed constant pressure ( $P = 0.56 \text{ atm}$ ). **c)** The exponents  $\alpha_c$  (empty circles) and  $\beta_c$  (black points), plotted as a function of the value of the imposed constant pressure. Note that as the pressure increases, the values of the exponents tend to those obtained in the case of constant pressure rate. The error bars represent the statistical uncertainty.

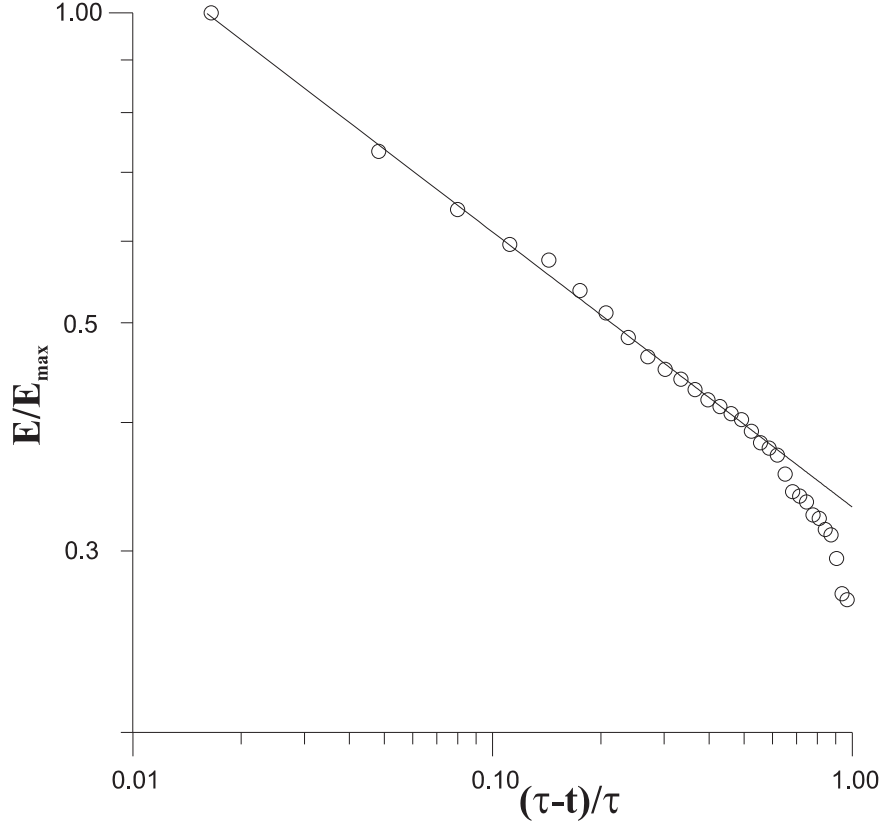


Figure 10: The cumulative energy  $E$ , normalized to  $E_{\max}$ , as a function of the reduced control parameter  $\frac{\tau-t}{\tau}$  at the neighborhood of the fracture point (Case of imposed constant pressure). The circles are the average for 9 wood samples. The solid line is the fit  $E = E_0 \left(\frac{\tau-t}{\tau}\right)^{-\gamma}$ . The exponent found,  $\gamma = 0.26$ , does not depend on the value of the imposed pressure. In the case of a constant pressure rate the same law has been found [10, 9].

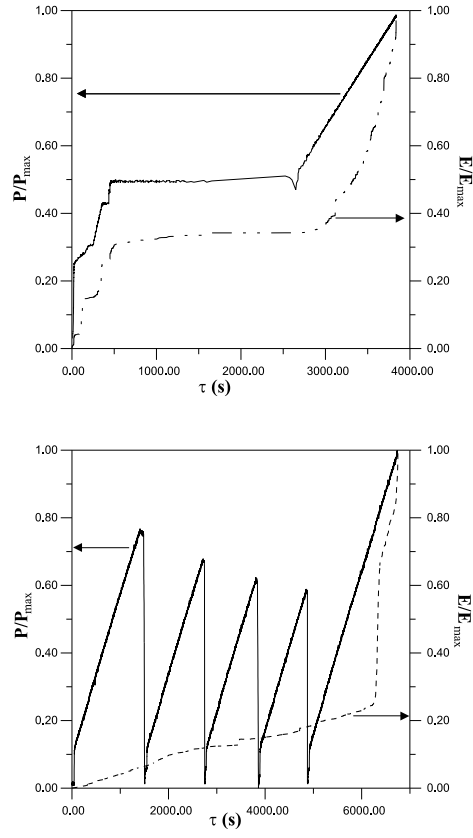


Figure 11: The imposed pressure, normalized at  $P_{\max}$ , (solid line) and the cumulative energy  $E$ , normalized to  $E_{\max}$ , (dashed line) are plotted as a function of time  $\tau$  a) An example of erratic pressure. b) A cyclic pressure.



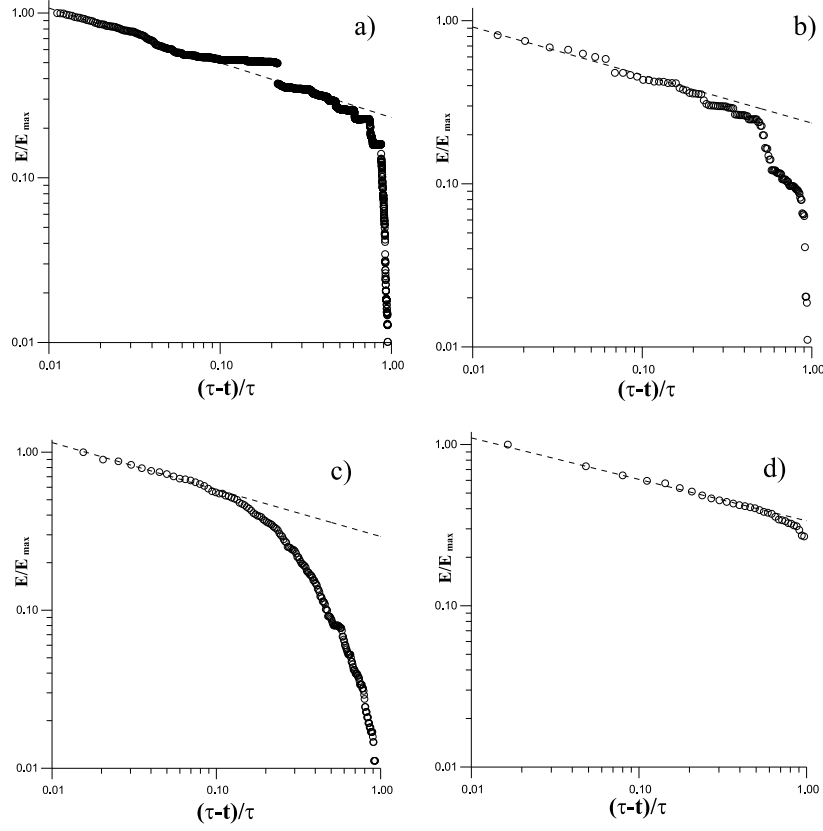


Figure 12: The cumulative energy  $E$ , normalized to  $E_{\max}$ , as a function of the reduced control parameter  $\frac{\tau-t}{\tau}$  at the neighborhood of the fracture point. Figure d) represent the measure taken, at imposed constant rate force, on the tensile machine. The other figures represent measures made on the HPC apparatus at : imposed constant pressure (c), imposed cyclic pressure (a) and imposed erratic pressure (b). The dotted lines are the fit  $E = E_0 \left( \frac{\tau-t}{\tau} \right)^{-\gamma}$ . The exponents found are:  $\gamma = 0.29$  (a),  $\gamma = 0.25$  (b),  $\gamma = 0.29$  (c) and  $\gamma = 0.27$  (d). In the case of a constant pressure rate (on the HPC machine) the same law has been found [10, 9]